Structural Engineering and Mechanics, *Vol. 73, No. 3 (2020) 259-269*
DOI: https://doi.org/10.12989/sem.2020.73.3.259

Bending analysis of thick functionally graded piezoelectric rectangular plates using higher-order shear and normal deformable plate theory

M. Lori Dehsaraji[1a], A.R. Saidi[2b] and M. Mohammadi*[1]

[1]*Department of Mechanical Engineering, Vali-e-Asr University of Rafsanjan, Rafsanjan, Iran*
[2]*Department of Mechanical Engineering, Shahid Bahonar University of Kerman, Kerman, Iran*

(Received March 3, 2019, Revised September 28, 2019, Accepted October 5, 2019)

Abstract. In this paper, bending-stretching analysis of thick functionally graded piezoelectric rectangular plates is studied using the higher-order shear and normal deformable plate theory. On the basis of this theory, Legendre polynomials are used for approximating the components of displacement field. Also, the effects of both normal and shear deformations are encountered in the theory. The governing equations are derived using the principle of virtual work and variational approach. It is assumed that plate is made of piezoelectric materials with functionally graded distribution of material properties. Hence, exponential function is used to modify mechanical and electrical properties through the thickness of the plate. Finally, the effect of material properties, electrical boundary conditions and dimensions are investigated on the static response of plate. Also, it is shown that results of the presented model are close to the three dimensional elasticity solutions.

Keywords: bending analysis; functionally graded; piezoelectric material; higher-order shear and normal deformable theory

1. Introduction

Functionally gradient piezoelectric materials (FGPMs), are composites made of piezoelectric materials that their material properties vary continuously along certain direction specially through the thickness. FGPMs are widely used in engineering applications, for example FGP actuators can produce large displacements while minimizing the internal stress concentrations, which will greatly improve the reliability and life of piezoelectric actuators.

Many researches have been done on 2-D analysis of plates, based on the classical, first order and third order shear deformation plate theories Reissner (1994), Mindlin *et al*. (1856), Reddy (1984) in accordance to their thickness ratio. In classical plate theory (CPT), normal and shear out of plane strains in the thickness direction are neglected, therefore this theory is usable for thin plates. In the first order shear deformation plate theory (FSDT), and the third order shear deformation theory (TSDT), shear deformations are considered but normal out of plane deformations are vanished. Thus, these theories are used for moderately thick plates.

For thick plate, three dimensional elasticity solutions give the best results but the solution process is difficult. The higher-order shear and normal deformable plate theory HOSNDPT) that was proposed by Batra and Vidoli (2002), (encounters all shear and normal strains in the thickness direction. Hence, this theory can be used for analysis of thick plates (Mohseni *et al*. (2017)). Batra (2007) developed the HOSNDPT for a plate comprised of a linear elastic incompressible anisotropic material. Sheikholeslami and Saidi (2013), used higher order shear and normal deformable plate theory for analyzing free vibration of functionally graded plates resting on elastic foundation exposed to simply support boundary condition, also they concluded results obtained of fifth-order HOSNDPT theory are similar to 3D elasticity theory.

Jadhav and Bajoria (2013) carried out stability analysis of functionally graded rectangular plates with piezoelectric actuators and sensors on the upper and lower surface. Nazari *et al*. (2011) applied element-free Galerkin method for studying the stress intensity factors of plates under thermal loading. They used continuum functions and the micromechanical model to describe the distribution of material properties. The effects of material initial residual stress and machining-induced residual stress on the deformation of aluminum alloy plate was studied by Huang *et al*. (2015).

Jam and Nia (2012) presented an exact solution for dynamic analysis of FGPM annular plate. A comprehensive overview of the higher-order theories was used by Wang and Yang (2000) to examine the dynamic behavior of piezoelectric plates. Static and dynamic behavior of carbon nanotube-reinforced composite plates resting on the Pasternak elastic foundation including shear layer and Winkler springs investigated by Wattanasakulponga and Chaikittiratanab (2015). Lim and Hi (2001) determined exact solution for compositionally graded piezoelectric layer under uniform stretch, bending and twisting. Free vibration analysis of functionally graded piezoelectric rectangular plates on the basis of three-dimensional

*Corresponding author, Professor
E-mail: meisam.mohammadi@vru.ac.ir
[a] M.Sc.
[b] Ph.D.

ISSN: 1225-4568 (Print), 1598-6217 (Online)

elasticity theory of transversely isotropic piezo-elasticity was shown by Chen and Ding (2012). Also they derived independent state equations with variable coefficients. Behjat and Khoshravan (2000) presented nonlinear bending and free vibration analysis of functionally graded piezoelectric plates by using finite element method under different sets of mechanical and electrical loadings.

Free vibration characteristics of laminated circular piezoelectric plates and discs were determined by Heyliger and Ramirez (2000). They used a discrete-layer model for the equations of periodic motion for both thin plates and for thick discs. Zhong and Shang (2003) used the theory of three-dimensional elasticity for bending of the functionally graded piezoelectric simply supported rectangular plate with different electrical boundary conditions. Lu *et al*. (2005) presented an exact solution for the cylindrical bending of the functionally graded piezoelectric plates. Furthermore, they discussed on the mechanical and electric properties of plates under mechanical and electrical forces. Zhong and Yu (2006) obtained an exact solution for free and forced vibrations of functionally graded piezoelectric simply supported rectangular plate with different electrical boundary conditions. Xiang and Shi (2009) presented static analysis of functionally graded piezoelectric sensors with combined thermal and electrical loadings. Behjat *et al*. (2011) showed static and dynamic analysis of functionally graded piezoelectric rectangular plates using first order shear deformation theory.

Bodaghi and Shakeri (2012) studied free vibration of functionally graded piezoelectric plates based on first-order shear theory. Intended vibration analysis of functionally graded piezoelectric shell based on the higher-order shear deformation theory was presented by Wu *et al*. (2002). Mohammadi *et al*. (2019) used HOSNDPT for investigating the effect of incompressibility on the behavior of thick plates.

In this paper, bending-stretching analysis of functionally graded piezoelectric plates is investigated for mechanical and electrical loadings, based on the higher order shear and normal plate theory. It is assumed that material properties vary through the thickness according to the exponential functions. Finally the static response of thick FGP plates are determined and compared to those of three dimensional elasticity solutions.

2. Constitutive relations based on the HOSNDPT

Consider a functionally grated piezoelectric (FGP) rectangular flat plate, with thickness h, length l_1 and width l_2. The FGP plate is transversely isotropic in x-y plane and also load $p(x, y)$ is exerted on the top surface of the plate (See Figure 1).

It is assumed that material properties of functionally graded piezoelectric plate vary continually in the thickness z direction based on the exponential function as Zhong and Shang (2003)

$$\Gamma(z)=\Gamma_0 e^{\left(N\left(\frac{1}{2}-\frac{z}{h}\right)\right)} \tag{1}$$

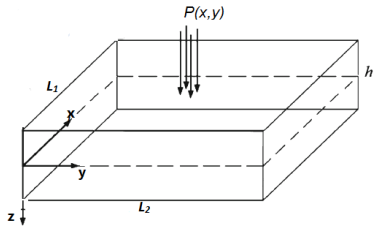

Fig. 1 Geometry of FGP rectangular plate

where, Γ indicates the typical material properties (electrical and mechanical), Γ_0 is the values of material properties at the bottom surface of plate, and N is the power index.

It is supposed that plate is thick enough so that three dimensional elasticity solutions must be applied for solving the problem. Due to the difficulty of three dimensional solutions, higher order shear and normal deformable plate theory, suggested by Batra and Vidoli (2002), is applied. It was shown that the results of this theory are close to the three dimensional elasticity solution but solution procedure is much simpler. In spite of the other classical plate theories, in higher order shear and normal deformable plate theory (HOSNDPT), all normal and shear strains are considered. According to the HOSNDPT, displacement field components are assumed as follows Batra (2007)

$$v_i(x,y,z)=v_\alpha(x,y,z)\delta_{i\alpha}+w(x,y,z)\delta_{i3} \quad i=1,2,3 \tag{2}$$

where v_i are the components of the total displacement, $w(x,y,z)$ is the out of plane displacements component, v_α are the components of in plane displacements, α shows directions of x or y and $\delta_{i\alpha}$ is the Kronecker delta. The displacement field components in z direction are approximated using orthogonal Legendre polynomial which are defined as Batra (2007)

$$\begin{aligned} v_\alpha(x,y,z)&=v_\alpha^a(x,y).L_a(z) \qquad \alpha=1,2 \\ w(x,y,z)&=w^a(x,y).L_a(z) \qquad a=0,1,2,...,K \end{aligned} \tag{3}$$

In equation (3), $L_a(z)$ are orthogonal Legendre terms with the following properties as

$$\begin{aligned} &\int_{-\frac{h}{2}}^{\frac{h}{2}} L_a(z)L_b(z)dz=\delta_{ab} \qquad a,b=0,1,2,...,K \\ &L_{n-1}(z)=\sqrt{\frac{(2n-1)}{h}}P_{n-1}(z) \qquad n\geq 1 \end{aligned} \tag{4}$$

where P is the basic polynomial which can be obtained by the following recursive function

$$\begin{aligned} &P_0(z)=1, \qquad P_1(z)=\frac{2z}{h} \\ &P_{n+1}(z)=\left(\frac{2n+1}{n+1}\right)\left(\frac{2z}{h}\right)P_n(z)-\left(\frac{n}{n+1}\right)P_{n-1}(z) \end{aligned} \tag{5}$$

In which K is the order of HOSNDPT theory.

Also, the derivation of Legendre polynomial is a linear combination of polynomials so that

$$L_a'(z)=D_{ab}L_b(z) \tag{6}$$

In equation (6), D is the matrix of derivation coefficients. For example for the fifth order theory, the components of this matrix can be written in the following form Batra (2007)

$$[D]=\frac{2}{h}\begin{bmatrix} 0 & 0 & 0 & 0 & 0 & 0 \\ \sqrt{3} & 0 & 0 & 0 & 0 & 0 \\ 0 & \sqrt{15} & 0 & 0 & 0 & 0 \\ \sqrt{7} & 0 & \sqrt{35} & 0 & 0 & 0 \\ 0 & 3\sqrt{3} & 0 & 3\sqrt{7} & 0 & 0 \\ \sqrt{11} & 0 & \sqrt{55} & 0 & 3\sqrt{11} & 0 \end{bmatrix} \tag{7}$$

For determining the constitutive relations, consider infinitesimal strain tensor components as

$$\varepsilon_{ij}=\frac{1}{2}\left(\frac{\partial v_i}{\partial x_j}+\frac{\partial v_j}{\partial x_i}\right) \tag{8}$$

The constitutive relation for piezoelectric material that are polarized in z direction is written as Askari Farsangi and Saidi (2012)

$$\begin{Bmatrix}\sigma_{xx}\\ \sigma_{yy}\\ \sigma_{zz}\\ \sigma_{yz}\\ \sigma_{xz}\\ \sigma_{xy}\end{Bmatrix}=-\begin{bmatrix} 0 & 0 & e_{31} \\ 0 & 0 & e_{31} \\ 0 & 0 & e_{33} \\ 0 & e_{15} & 0 \\ e_{15} & 0 & 0 \\ 0 & 0 & 0 \end{bmatrix}\begin{Bmatrix}E_x\\ E_y\\ E_z\end{Bmatrix} + \begin{bmatrix} C_{11} & C_{12} & C_{13} & 0 & 0 & 0 \\ C_{12} & C_{11} & C_{13} & 0 & 0 & 0 \\ C_{13} & C_{13} & C_{33} & 0 & 0 & 0 \\ 0 & 0 & 0 & C_{55} & 0 & 0 \\ 0 & 0 & 0 & 0 & C_{55} & 0 \\ 0 & 0 & 0 & 0 & 0 & \frac{1}{2}(C_{11}-C_{12}) \end{bmatrix}\begin{Bmatrix}\varepsilon_{xx}\\ \varepsilon_{yy}\\ \varepsilon_{zz}\\ \gamma_{yz}\\ \gamma_{xz}\\ \gamma_{xy}\end{Bmatrix} \tag{9}$$

and the components of the electric displacements of the plate are

$$\begin{Bmatrix}D_x\\ D_y\\ D_z\end{Bmatrix}=\begin{bmatrix}\lambda_{11} & 0 & 0\\ 0 & \lambda_{11} & 0\\ 0 & 0 & \lambda_{33}\end{bmatrix}\begin{Bmatrix}E_x\\ E_y\\ E_z\end{Bmatrix} + \begin{bmatrix} 0 & 0 & 0 & 0 & e_{15} & 0 \\ 0 & 0 & 0 & e_{15} & 0 & 0 \\ e_{31} & e_{31} & e_{33} & 0 & 0 & 0 \end{bmatrix}\begin{Bmatrix}\varepsilon_{xx}\\ \varepsilon_{yy}\\ \varepsilon_{zz}\\ \gamma_{yz}\\ \gamma_{xz}\\ \gamma_{xy}\end{Bmatrix} \tag{10}$$

where σ_{ij} are the stress components, D_i are the electric displacement components, ε_{ij} are the strain components, C_{ij} are the elastic stiffness components, e_{ij} are the piezoelectric components, $\lambda_{ij}=\frac{1}{2}\left(\frac{\partial v_i}{\partial x_j}+\frac{\partial v_j}{\partial x_i}\right)$ are the dielectric components and $E_i(V/m)$ are the electric field components. The electric filed vector is related to the gradient of electric potential function Φ, as

$$\mathbf{E}=-\nabla\Phi \tag{11}$$

3. Governing equations of plate

Consider the equilibrium equations in Cartesian coordinate as

$$\sigma_{ij,j}+\rho b_i=0 \tag{12}$$

where ρ is the plate density and b_i are the components of body force vector. The principle of virtual work is used to obtain the governing equations. Suppose a small virtual displacement field $\delta\eta_i$. Taking the inner product of equation (12) leads to

$$\int\int_{-h/2}^{h/2}\delta\eta_i\sigma_{ij,j}dzdA+\int\int_{-h/2}^{h/2}\rho\delta\eta_i b_i dzdA=0 \qquad i=1,2,3 \tag{13}$$

Also, the virtual displacement components are expanded utilizing the Legendre polynomial as

$$\delta\eta_i(x,y,z)=L_a(z)\delta\eta_i^a(x,y) \tag{14}$$

Substituting equation (14) in to equation (13) and using equations (2) and (6) results in

$$\int_A\delta\eta_\alpha^a M_{\alpha\beta,\beta}^a dA+\int_A\delta\eta_3^a T_{\alpha,\alpha}^a dA+\int_A\delta\eta_i^a\left(b_i^a+B_i^a-D_{ab}T_i^b\right)dA=0 \tag{15}$$

The resultant forces and moments in the above equation are defined as

$$\begin{aligned} &M_{\alpha\beta}^a=\int_{-h/2}^{h/2}\sigma_{\alpha\beta}L_a dz \qquad T_i^a=\int_{-h/2}^{h/2}\sigma_{i3}L_a dz \\ &B_i^a=L_a(\frac{h}{2})\sigma_{i3}(x,y,\frac{h}{2})-L_a(-\frac{h}{2})\sigma_{i3}(x,y,-\frac{h}{2}) \\ &b_i^a=\int_{-\frac{h}{2}}^{\frac{h}{2}}\rho L_a b_i\,dz \end{aligned} \tag{16}$$

Simplifying equation (15) and implementing the Maxwell's equation for satisfying the electrical properties of FGP plate leads to

$$\begin{aligned} &M_{\alpha\beta,\beta}^a+b_\alpha^a+B_\alpha^a-D_{ab}T_\alpha^b=0 \\ &T_{\alpha,\alpha}^a+b_3^a+B_3^a-D_{ab}T_3^b=0 \qquad \alpha,\beta=1,2 \\ &\int_{-\frac{h}{2}}^{\frac{h}{2}}\vec{\nabla}.\vec{D}dz=\int_{-\frac{h}{2}}^{\frac{h}{2}}(D_{x,x}+D_{y,y}+D_{z,z})dz=0 \end{aligned} \tag{17}$$

In the above equation, $M_{\alpha\beta}^0$ are in plane forces, $M_{\alpha\beta}^1$ are out of plane first moment, $M_{\alpha\beta}^0$ are out of plane moments with the order of a, T_i^0 are resultant of lateral forces, T_i^1 are first moment of transverse force, T_i^a are moment of transverse force with the order of a, b_i^0 are body forces per unit area, b_i^1 are first moment of body forces per unit area, b_i^a are moment of body forces per unit area with the order of a, B_i^a are moment of surface stresses on the top and bottom surfaces of the plate with the order of a.

Also, the corresponding boundary conditions are

$$\begin{aligned} &\sigma_z\left(z=-h/2\right)=-P(x,y) \qquad &&\sigma_z\left(z=+h/2\right)=0 \\ &\tau_{xz}\left(z=\pm h/2\right)=0 \qquad &&\tau_{yz}\left(z=\pm h/2\right)=0 \end{aligned} \tag{18}$$

Also, neglecting the volume forces, body forces in relation (16) are simplified as

$$b_1^a = b_2^a = b_3^a = 0 \qquad B_1^a = 0$$
$$B_2^a = 0 \qquad B_3^a = L_a(-\frac{h}{2})\, P(x,y) \tag{19}$$

Consider a general form of the electrical potential field Zheng and Tao (2006)

$$\Phi(x,y,z) = A(x,y)z + B(x,y) + \phi(x,y)\left[1-\left(\frac{2z}{h}\right)^2\right] \tag{20}$$

Where the unknown functions $A(x,y)$ and $B(x,y)$ are derived from electrical boundary conditions of the plate. Expanding equations (17) for α,β =1,2 and also using the constitutive equations (9), general form of governing equilibrium equations for FGP plate are obtained as

$$\begin{aligned}
&\int_{-\frac{h}{2}}^{\frac{h}{2}} L_a L_c C_{11}\left[v^c_{1,11} + \frac{1}{2}\left(v^c_{1,22} + v^c_{2,12}\right)\right]dz \\
&+\int_{-\frac{h}{2}}^{\frac{h}{2}} L_a L_c C_{12}\left[\frac{1}{2}\left(v^c_{2,21} - v^c_{1,22}\right)\right]dz \\
&+D_{dc}\int_{-\frac{h}{2}}^{\frac{h}{2}} L_a L_c C_{13}dz\left[w^d_{,1}\right] - \int_{-\frac{h}{2}}^{\frac{h}{2}} L_a e_{31}\left[-A_{,1} + \frac{8z}{h^2}\phi_{,1}\right]dz \\
&-D_{ab}\int_{-\frac{h}{2}}^{\frac{h}{2}} L_b L_d C_{55}dz\left[D_{cd}v^c_1 + w^d_{,1}\right] \\
&-D_{ab}\int_{-\frac{h}{2}}^{\frac{h}{2}} L_b e_{15}\left[A_{,1}z + B_{,1} + \left(1-\left(\frac{2z}{h}\right)^2\right)\phi_{,1}\right]dz = 0
\end{aligned} \tag{21a}$$

$$\begin{aligned}
&\int_{-\frac{h}{2}}^{\frac{h}{2}} L_a L_c C_{11}\left[\frac{1}{2}\left(v^c_{1,21} + v^c_{2,11}\right) + v^c_{2,22}\right]dz \\
&+\int_{-\frac{h}{2}}^{\frac{h}{2}} L_a L_c C_{12}\left[\frac{1}{2}\left(v^c_{1,12} - v^c_{2,11}\right)\right]dz \\
&+D_{dc}\int_{-\frac{h}{2}}^{\frac{h}{2}} L_a L_c C_{13}dz\left[w^d_{,2}\right] - \int_{-\frac{h}{2}}^{\frac{h}{2}} L_a e_{31}\left[-A_{,2} + \frac{8z}{h^2}\phi_{,2}\right]dz \\
&-D_{ab}\int_{-\frac{h}{2}}^{\frac{h}{2}} L_b L_d C_{55}dz\left[D_{cd}v^c_2 + w^d_{,2}\right] \\
&-D_{ab}\int_{-\frac{h}{2}}^{\frac{h}{2}} L_b e_{15}\left[A_{,2}z + B_{,2} + \left(1-\left(\frac{2z}{h}\right)^2\right)\phi_{,2}\right]dz = 0
\end{aligned} \tag{21b}$$

$$\begin{aligned}
&\int_{-\frac{h}{2}}^{\frac{h}{2}} L_a L_d C_{55}\left[D_{cd}\left(v^c_{1,1} + v^c_{2,2}\right) + \nabla^2 w^d\right]dz \\
&+\int_{-\frac{h}{2}}^{\frac{h}{2}} L_a e_{15}\left[\nabla^2 A z + \nabla^2 B + \left(1-\left(\frac{2z}{h}\right)^2\right)\nabla^2\phi\right]dz \\
&-D_{ab}\int_{-\frac{h}{2}}^{\frac{h}{2}} L_b L_c C_{13}dz\left[v^c_{1,1} + v^c_{2,2}\right] - D_{ab}\int_{-\frac{h}{2}}^{\frac{h}{2}} L_b L_c C_{33}dz\left[D_{cd}w^d\right] \\
&+D_{ab}\int_{-\frac{h}{2}}^{\frac{h}{2}} L_b e_{33}\left[-A + \frac{8z}{h^2}\phi\right]dz + P(x,y)L_a(\tfrac{-h}{2}) = 0
\end{aligned} \tag{21c}$$

$$\begin{aligned}
&\int_{-\frac{h}{2}}^{\frac{h}{2}} L_d e_{15}\left[D_{cd}\left(v^c_{1,1} + v^c_{2,2}\right) + \nabla^2 w^d\right]dz \\
&-\int_{-\frac{h}{2}}^{\frac{h}{2}} \lambda_{11}\left[\nabla^2 Az + \nabla^2 B + \left(1-\left(\frac{2z}{h}\right)^2\right)\nabla^2\phi\right]dz \\
&+D_{cd}\int_{-\frac{h}{2}}^{\frac{h}{2}} L_d e_{13}dz\left[v^c_{1,1} + v^c_{2,2}\right] + \int_{-\frac{h}{2}}^{\frac{h}{2}} L_c\frac{\partial e_{13}}{\partial z}dz\left[v^c_{1,1} + v^c_{2,2}\right] \\
&+D_{bc}\int_{-\frac{h}{2}}^{\frac{h}{2}} L_c e_{33}dz\left[D_{db}w^d\right] + \int_{-\frac{h}{2}}^{\frac{h}{2}} \lambda_{33}dz\left[\frac{8}{h^2}\phi\right] \\
&+\int_{-\frac{h}{2}}^{\frac{h}{2}} L_c\frac{\partial e_{33}}{\partial z}dz\left[D_{dc}w^d\right] + \int_{-\frac{h}{2}}^{\frac{h}{2}} \frac{\partial \lambda_{33}}{\partial z}\left[-A + \frac{8z}{h^2}\phi\right]dz = 0
\end{aligned} \tag{21d}$$

Equations (21) are coupled in terms of displacement field and also electrical potential field. The unknown functions $A(x,y)$ and $B(x,y)$ are determined according to the different electrical boundary conditions. Three cases of electrical boundary conditions are considered.

Case 1, Closed circuit: It is assumed that both surfaces of FGP plate are short connected, or connected to the same voltage. Hence, the electrical boundary conditions on the plate surfaces can be written as

$$\Phi\left(z = \pm\frac{h}{2}\right) = 0 \tag{22}$$

Replacing boundary conditions (22) in equation (20), unknown functions $A(x,y)$ and $B(x,y)$ are obtained to be zero. Thus, the electric potential is determined as

$$\Phi(x,y,z) = \phi(x,y)\left[1-\left(\frac{2z}{h}\right)^2\right] \tag{23}$$

Case 2, Open-closed circuit: In this state, it is supposed that zero voltage is applied to the bottom surface of plate and the upper surface is insulated. So, the electrical boundary conditions on the plate surfaces can be written as

$$\Phi\left(z = -\frac{h}{2}\right) = 0, D_z\left(z = +\frac{h}{2}\right) = 0 \tag{24}$$

Upon substituting the prescribed boundary conditions (24) in equation (18), unknown functions $A(x,y)$ and $B(x,y)$ are

$$\begin{aligned}
A(x,y) &= \frac{1}{\lambda_{33}\left(\frac{h}{2}\right)} \\
&\left[e_{31}\left(\frac{h}{2}\right)L_c\left(\frac{h}{2}\right)\left[v^c_{1,1} + v^c_{2,2}\right] + e_{33}\left(\frac{h}{2}\right)L_c\left(\frac{h}{2}\right)\left[D_{dc}w^d\right] + \frac{4}{h}\phi\right] \\
B(x,y) &= \mathrm{A}(x,y).(\frac{h}{2})
\end{aligned} \tag{25}$$

Case 3, Electrical loading: In this case, it is assumed that no transverse mechanical load is applied to the plate ($\sigma_3|_{z=\pm h/2} = 0$), but sinusoidal voltage is applies on the top surface of the plate and the bottom surface of the plate is electrically insulated. Thus the electrical boundary conditions on the plate surfaces can be written as follows

$$\Phi\left(z=-\frac{h}{2}\right)=\sin\left(\frac{\pi x}{l_1}\right)\sin\left(\frac{\pi y}{l_2}\right), D_z\left(z=\frac{h}{2}\right)=0 \tag{26}$$

Using equations (26) and equation (20), the functions $A(x,y)$ and $B(x,y)$ are determined so that

$$A(x,y)=\frac{1}{\lambda_{33}\left(\frac{h}{2}\right)}\Bigg[e_{31}\left(\frac{h}{2}\right)L_c\left(\frac{h}{2}\right)\left[v_{1,1}^c+v_{2,2}^c\right] +e_{33}\left(\frac{h}{2}\right)L_c\left(\frac{h}{2}\right)\left[D_{dc}w^d\right]+\frac{4}{h}\phi\Bigg] \tag{27}$$

$$B(x,y)=A(x,y).(\frac{h}{2}).\sin\left(\frac{\pi x}{l_1}\right)\sin\left(\frac{\pi y}{l_2}\right)$$

4. Navier solution

In order to have exact and analytical solution, it is supposed that FGP plate is simply supported along all edges and is subjected to the mechanical distributed load P_0 is applied on it's the top surfaces.

Using the variational approach and divergence theorem, the boundary conditions are also determined. For simply supported edges, they are

$$\begin{aligned} &w^a=0, M_{11}^a=0, M_{12}^a=0 && on?x=\ l_1\\ &w^a=0, M_{22}^a=0, M_{12}^a=0 && on?y=\ l_2 \end{aligned} \tag{28}$$

For plates with all edges simply supported, Navier solution is used and the functions are approximated by double trigonometric Fourier series. Therefore,

$$\begin{aligned} v_1^a &= \sum_{m=1,3,5}^{\infty}\sum_{n=1,3,5}^{\infty} v_1^{amn}\cos\left(\frac{m\pi x}{l_1}\right)\sin\left(\frac{n\pi y}{l_2}\right)\\ v_2^a &= \sum_{m=1,3,5}^{\infty}\sum_{n=1,3,5}^{\infty} v_1^{amn}\sin\left(\frac{m\pi x}{l_1}\right)\cos\left(\frac{n\pi y}{l_2}\right)\\ w^a &= \sum_{m=1,3,5}^{\infty}\sum_{n=1,3,5}^{\infty} w^{amn}\sin\left(\frac{m\pi x}{l_1}\right)\sin\left(\frac{n\pi y}{l_2}\right)\\ P_0 &= \sum_{m=1,3,5}^{\infty}\sum_{n=1,3,5}^{\infty} \frac{16P_0}{mn\pi^2}\sin\left(\frac{m\pi x}{l_1}\right)\sin\left(\frac{n\pi y}{l_2}\right)\\ \phi(x,y) &= \tilde{\varphi}^{mn}\sum_{m=1,3,5}^{\infty}\sum_{n=1,3,5}^{\infty}\sin\left(\frac{m\pi x}{l_1}\right)\sin\left(\frac{n\pi y}{l_2}\right) \end{aligned} \tag{29}$$

It is easy to show that the above displacement components satisfy boundary conditions (28). Upon substituting the solutions (29) in the equilibrium equations (21) and also considering the Fourier expansion for the functions $A(x,y)$ and $B(x,y)$, a set of four algebraic equations are determined, which are given in appendix A. It is easy to show that, depending on the order of theory (K), number of algebraic equations is ($3K$+4).

Table 1 Comparison of stresses and transverse displacement

	$W*10^{-10}(m)$		$V_1*10^{-11}(m)$		$\sigma_x\,(Pa)$	
N	3D elasticity solution Zhong and Shang (2003)	Present study	3D elasticity solution Zhong and Shang (2003)	Present study	3D elasticity solution Zhong and Shang (2003)	Present study
-1	2.5100	2.5100	-3.0377	-3.0860	15.3323	15.3821
-0.5	1.9250	1.9298	-2.6192	-2.6379	12.9991	13.0293
0	1.4825	1.4947	-2.2008	-2.2604	10.9992	10.9491
0.5	1.1600	1.1705	-1.8661	-1.9416	9.1660	9.21398
1	0.9125	0.9239	-1.6151	-1.6637	7.6661	7.6832

Table 2 Convergence of results for the plate center deflection

(h/l_1)	N	K=1	K=2	K=3	K=4	K=5
0.01	-3	2.3086	2.9849	2.9848	2.9848	2.9848
	-2	1.3507	1.6940	1.6940	1.6940	1.6940
	0	0.4715	0.5630	0.5630	0.5630	0.5630
	2	0.1829	0.2293	0.2293	0.2293	0.2293
0.1	-3	2.3944	3.0325	3.0312	3.0099	3.0329
	-2	1.4192	1.7385	1.7439	1.7286	1.7433
	0	0.5051	0.5877	0.59239	0.5910	0.5910
	2	0.1954	0.2402	0.2411	0.2400	0.24097
0.2	-3	2.6612	3.173	3.1689	3.0717	3.1750
	-2	1.6257	1.8698	1.8921	1.8230	1.8890
	0	0.6042	0.6614	0.67407	0.6740	0.68022
	2	0.2321	0.2772	0.2761	0.2714	0.2754
0.5	-3	4.4577	4.1268	4.1119	3.9628	4.0971
	-2	2.9394	2.6930	2.8598	2.0501	2.7778
	0	1.2026	1.1299	1.2453	1.1844	1.18504
	2	0.4515	0.4702	0.4877	0.4791	0.47818

Table 3 Dimensionless parameters of displacements and stress for different thickness ratios and different powers, (K=5), closed circuit

(h/l_1)	N	$\bar{w}$	$\bar{v}_1$	$\overline{\sigma_x}$	$\overline{\tau_{xy}}$	$\overline{\sigma_z}$	$\overline{\tau_{xz}}$
0.1	0	0.59100	-0.1670	-1.0276	0.27814	-0.08413	0.11563
	1	0.37156	-0.1338	-0.9254	0.20925	-0.07523	0.13507
	2	0.24097	-0.1522	-0.7179	0.10806	-0.07151	0.1547
	3	0.15530	-0.1300	-0.3923	-0.0366	-0.06721	0.17398
0.2	0	0.67407	-0.1345	-0.5162	0.12128	-0.14315	0.10543
	1	0.42768	-0.3262	-0.4731	0.08514	-0.1500	0.1341
	2	0.2754	-0.3382	-0.3625	0.03239	-0.1437	0.15389
	3	0.17483	-0.2783	-0.1887	-0.0427	-0.13516	0.17328
0.3	0	0.80667	-0.4554	-0.3808	0.0590	-0.25975	0.1096
	1	0.5173	-0.6313	-0.32866	0.03505	-0.22501	0.13046
	2	0.32984	-0.5862	-0.24593	-0.00254	-0.21762	0.15164
	3	0.20532	-0.4584	-0.11786	-0.05571	-0.20385	0.17242
0.5	0	1.1850	-2.1022	-0.2601	-0.0068	-0.43124	0.10233
	1	0.77152	-1.7646	-0.2309	-0.0200	-0.40842	0.12678
	2	0.47818	-1.3456	-0.1535	-0.0484	-0.37102	0.15304
	3	0.28529	-0.9404	-0.0547	-0.0855	-0.33646	0.17743

5. Numerical results

In order to have a numerical study, it is assumed that the bottom surface of FGP plate is made of PZT-4 with the following material properties Zhang and Shang (2003), Askari Farsangi and Saidi (2013)

$$\begin{aligned}&\text{Elastic moduli :}\\&C_{11}=139\ GPa,\ C_{12}=77.8\ GPa,\ C_{13}=74.3\ GPa,\\&C_{33}=115\ GPa,\ C_{55}=25.6\ GPa\\&\text{Piezoelectric moduli :}\\&e_{15}=12.7\left(c.m^{-2}\right),\ e_{31}=-5.2\left(c.m^{-2}\right),\ e_{33}=15.1\left(c.m^{-2}\right)\\&\text{Dielectric moduli :}\\&\lambda_{11}=6.46\ *10^{-9}(F.m^{-2}),\ \lambda_{33}=5.62\ *10^{-9}(F.m^{-2})\end{aligned}\tag{30}$$

For validation of the results, a comparison is done in Table 1, with three dimensional elasticity solution results presented by Zhong and Shang (2003) for a functionally graded piezoelectric plate (h/l_1=0.1). Sinusoidal transverse electrical load with unit amplitude is exerted on the plate surface and closed circuit electrical condition is considered. Comparison shows that there is a good agreement between the presented solution and results of three dimensional elasticity solution.

For simplicity and also keeping the generality, results are normalized as

$$\begin{aligned}&\bar{w}=w\left(\frac{l_1}{2},\frac{l_2}{2},0\right)\frac{(C_{11}^{PZT-4})h^3}{P_0{l_1}^4}*10,\quad \bar{\sigma}_x=\sigma_x\left(\frac{l_1}{2},\frac{l_2}{2},\frac{-h}{4}\right)\frac{h}{P_0l_1}\\&\bar{\sigma}_y=\sigma_y\left(\frac{l_1}{2},\frac{l_2}{2},\frac{-h}{4}\right)\frac{h}{P_0l_1},\qquad \bar{\tau}_{xy}=\tau_{xy}\left(0,0,\frac{-h}{4}\right)\frac{h}{P_0l_1}\\&\tau_{xz}\left(0,\frac{l_2}{2},\frac{-h}{4}\right)\frac{h}{P_0l_1},\qquad \bar{\tau}_{yz}=\tau_{yz}\left(\frac{l_1}{2},0,\frac{-h}{4}\right)\frac{h}{P_0l_1}\\&\bar{v}_1=v_1\left(0,\frac{l_2}{2},0\right)\frac{(C_{11}^{PZT-4})h^3}{P_0{l_1}^4}*100\end{aligned}\tag{31}$$

Table 4 Dimensionless parameters of displacements and stress for different thickness ratios and different powers, (K=5) open-closed circuit

(h/l_1)	N	$\bar{w}$	$\bar{v}_1$	$\bar{\sigma}_x$	$\bar{\tau}_{xy}$	$\bar{\sigma}_z$	$\bar{\tau}_{xz}$
0.01	0	0.5630	-0.00002	-10.1347	2.9064	-0.0084	0.1152
	1	0.3442	-0.0094	-8.816	2.5278	-0.0080	0.1347
	2	0.2129	-0.01116	-6.4225	1.8409	-0.0076	0.1545
	3	0.1318	-0.0096	-2.7846	0.7969	-0.0071	0.1738
0.1	0	0.5909	-0.0184	-1.0288	0.2774	-0.0841	0.1156
	1	0.3645	-0.1063	-0.896	0.2374	-0.0804	0.1350
	2	0.2264	-0.1187	-0.6516	0.1664	-0.0762	0.1547
	3	0.1400	-0.1007	-0.2804	0.0591	-0.0714	0.1740
0.2	0	0.6733	-0.1461	-0.5375	0.1189	-0.1696	0.1146
	1	0.4236	-0.2844	-0.4693	0.0957	-0.1619	0.1342
	2	0.2654	-0.2826	-0.3396	0.0566	-0.1529	0.1541
	3	0.1636	-0.2282	-0.1428	-0.0015	-0.1429	0.1736

Table 5 Displacements and stresses for different dimension ratios and different thickness ratios, (K=5), electrical loading

l_1/l_2	(h/l_1)	$W\ *10^{-10}(m)$	$V_1*10^{-10}(m)$	$\sigma_x\ (Pa)$	$\tau_{xy}\ (Pa)$
1	0.1	3.9034	0.1354	8.9795	8.8198
	0.2	-3.4893	0.2393	17.0505	15.908
	0.5	-1.8367	0.33145	32.8716	23.303
2	0.1	-3.6869	0.12711	34.407	16.7321
	0.2	-2.8452	0.1934	58.88	26.52
	0.5	-0.6766	0.2190	82.004	27.168
3	0.1	-3.3669	0.1151	72.746	23.101
	0.2	-2.1083	0.1473	110.569	31.047
	0.5	0.14618	0.1774	123.06	25.8216

For simplicity and also keeping the generality, results are normalized as

$$\begin{aligned}&\bar{w}=w\left(\frac{l_1}{2},\frac{l_2}{2},0\right)\frac{(C_{11}^{PZT-4})h^3}{P_0{l_1}^4}*10,\quad \bar{\sigma}_x=\sigma_x\left(\frac{l_1}{2},\frac{l_2}{2},\frac{-h}{4}\right)\frac{h}{P_0l_1}\\&\bar{\sigma}_y=\sigma_y\left(\frac{l_1}{2},\frac{l_2}{2},\frac{-h}{4}\right)\frac{h}{P_0l_1},\qquad \bar{\tau}_{xy}=\tau_{xy}\left(0,0,\frac{-h}{4}\right)\frac{h}{P_0l_1}\\&\tau_{xz}\left(0,\frac{l_2}{2},\frac{-h}{4}\right)\frac{h}{P_0l_1},\qquad \bar{\tau}_{yz}=\tau_{yz}\left(\frac{l_1}{2},0,\frac{-h}{4}\right)\frac{h}{P_0l_1}\\&\bar{v}_1=v_1\left(0,\frac{l_2}{2},0\right)\frac{(C_{11}^{PZT-4})h^3}{P_0{l_1}^4}*100\end{aligned}\tag{32}$$

Table (2) shows the convergence of solution for the dimensionless central deflection of FGP square plate for the case of closed circuit. Results are given for different power index and different thickness ratio.

According to the table, it is clear that for thin plates, results converge rapidly and for the thicker plates results converge for K=5 and it is suitable for analysis. In Tables 3 and 4, central deflections and also different stresses (normal and shear) for thick FGP plate are tabulated for close and open-closed circuits, respectively. According to the tables, increasing the thickness ratio increases the dimensionless central deflection. In addition, increasing the power index increases the flexural rigidity of FGP plate.

Table 5 presents the static response of FGP plate (N=2) subjected the case of sinusoidal loading. It is seen from the table that variation of thickness and central deflection has an inverse relation, but the in-plane normal and shear stresses and also in-plane displacement have direct relationship.

Figures 2 and 3, show variation of dimensionless central deflection versus the length to thickness ratio and aspect ratio, respectively. Closed circuit electrical condition is considered and also the effect of power index N is investigated.

According to the figures 2 and 3, increasing the power index decreases the normalized central deflection. This variation is more apparent for the smaller values for aspect ratio and length to thickness ratio.

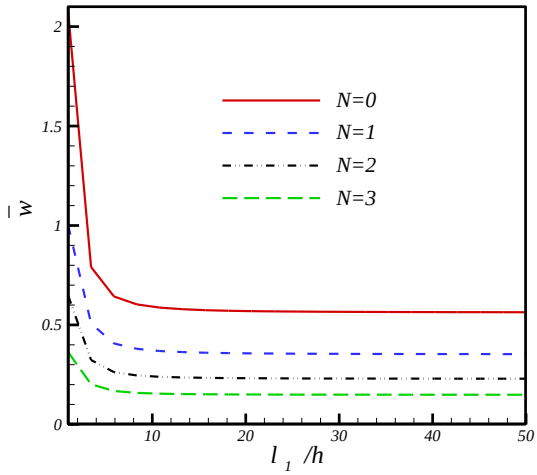

Fig. 2 Variation of the dimensionless central deflection respect to (l_1/h) for different power index

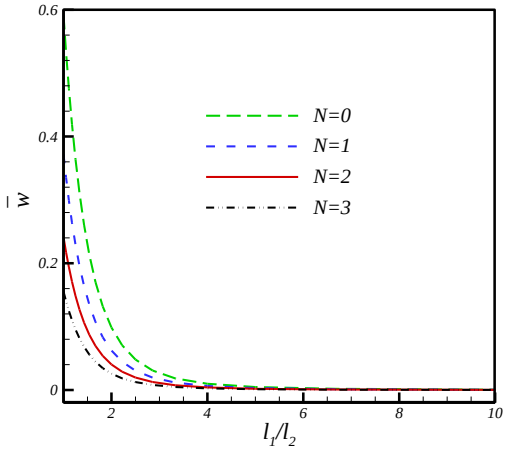

Fig. 3 Variation of the normalized central deflection versus to (l_1/l_2) for different power index

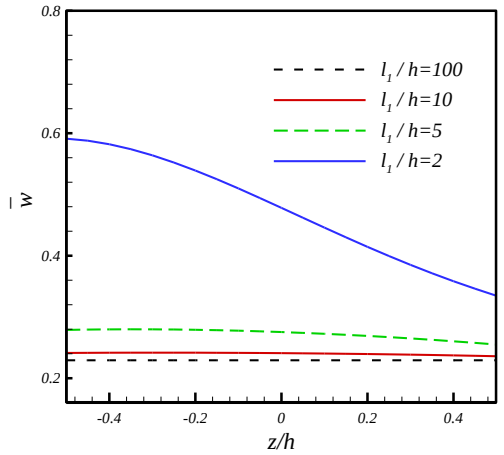

Fig. 4 Distribution of dimensionless central deflection along the thickness of FGP plate

Figure 4 shows variation of dimensionless central deflection along the thickness versus different the thickness ratios for closed circuit state. It is clear that variation is more apparent for thick plates.

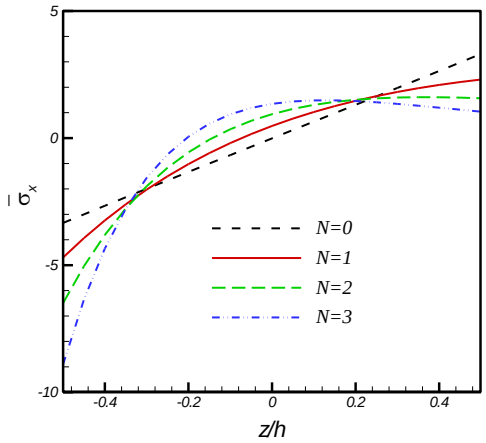

Fig. 5 Distribution of in-plane normal stress along the thickness for different power indices of square FGP plate

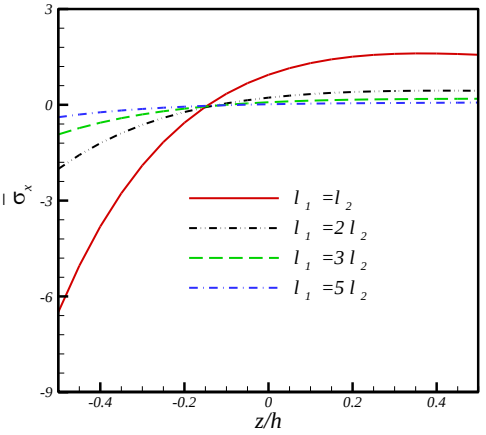

Fig. 6 Variation of in-plane normal stress along the thickness for different aspect ratios

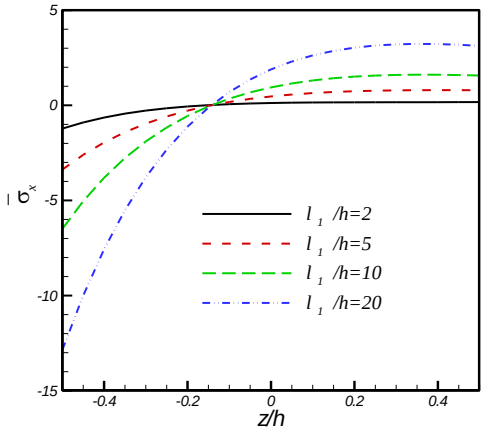

Fig. 7 Differences of in-plane normal stress along the thickness for different thickness ratios.

Figures 5, 6 and 7 show distribution of in-plane dimensionless normal stress along the thickness of the FGP plate versus change in different plate's parameters. Also, Figures 8 and 9 show distribution of in-plane dimensionless shear stress along the thickness of the plate for different thickness ratios and different aspect ratios, respectively. In addition, case of closed circuit electrical condition is considered.

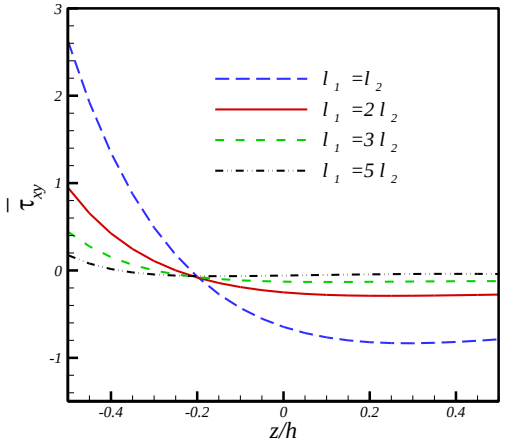

Fig. 8 In-plane shear stress differences along the thickness for different aspect ratios

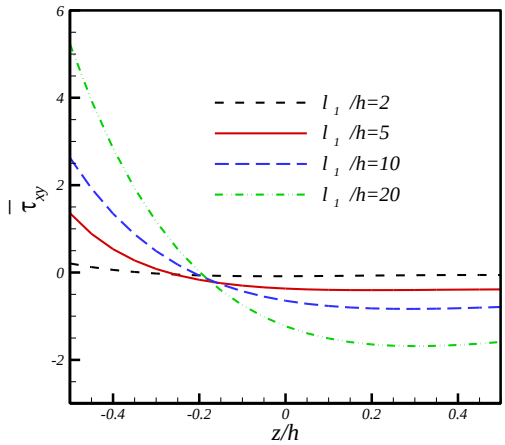

Fig. 9 In-plane shear stress distributions along the thickness for different thickness ratios

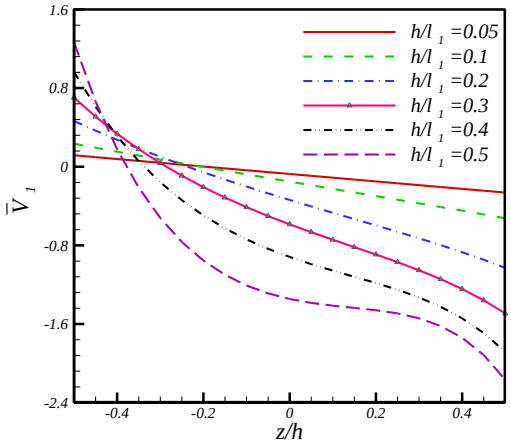

Fig. 10 In-plane displacement differences along the thickness for different thickness ratios

Figure 10 shows variation of in-plane displacement along the thickness of FGP plate for different thickness ratios in case closed circuit. Effect of aspect ratio on the out of plane dimensionless shear stress along the thickness of FGP plate is depicted in figure 10. Closed circuit electrical condition is considered. Reviewing figures 6 to 11 indicates

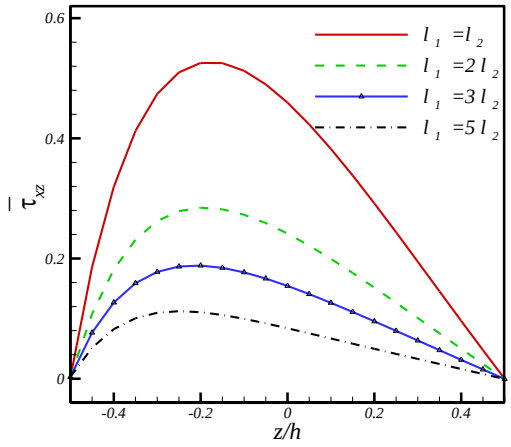

Fig. 11 Out of-plane shear stress variation along the thickness for different aspect ratios

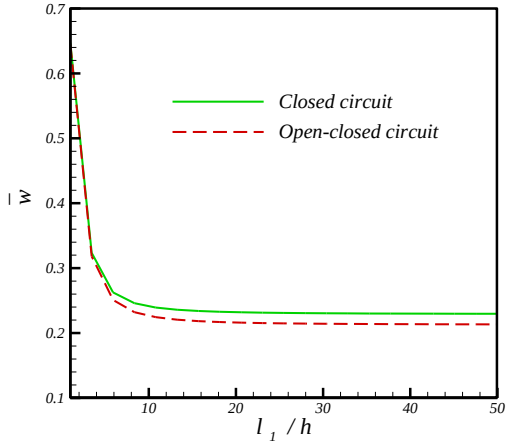

Fig. 12 Effect of elec1trical boundary conditions on the dimensionless central

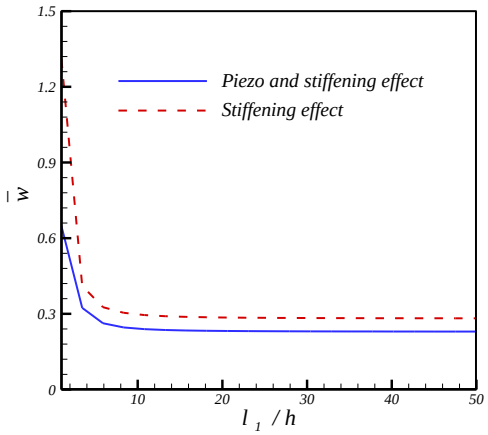

Fig. 13 Influence of piezoelectric properties on the plate central deflection

that values of normalized normal and shear stresses are zero not on the symmetric plane in the thickness direction. According to the numerical results, they are zero on ($z = -0.15h$), therefore, for the considered FGP plate, neutral plane does not coincide with the mid-plane and it locates in different coordinate.

In Figure 12, effect of electrical boundary conditions on the dimensionless central deflection of FGP plate is plotted.

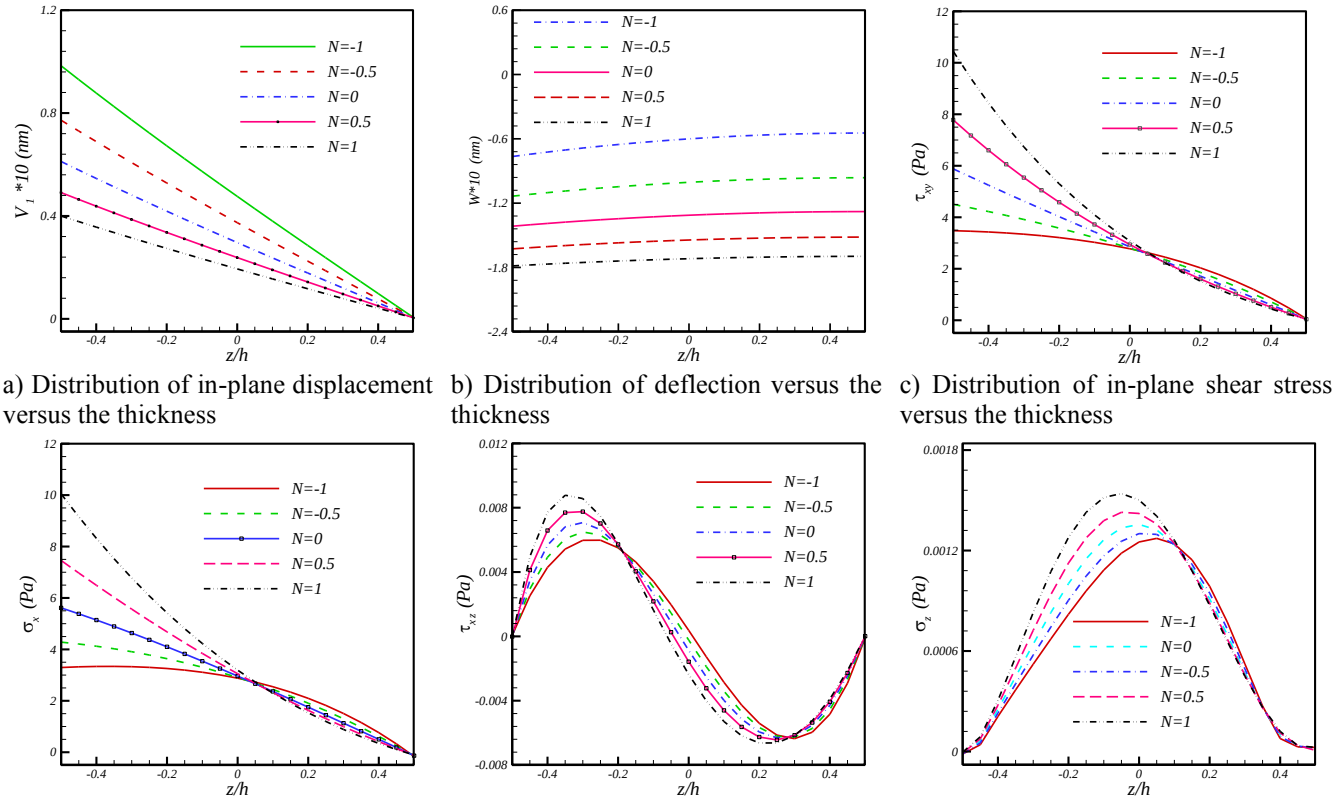

a) Distribution of in-plane displacement versus the thickness

b) Distribution of deflection versus the thickness

c) Distribution of in-plane shear stress versus the thickness

d) Distribution of in-plane normal stress versus the thickness

e) Distribution of out of plane shear stress versus the thickness

f) Distribution of out of plane normal stress versus the thickness

Fig. 14 Effect of electrical loading on the static responses of FGP plate (l_1/4,l_2/4,z)

In order to investigate the piezoelectric effect on the plate deflection, in Figure 13, normalized central deflection is plotted for FG plate with piezoelectric and without piezo electric properties. It is clear that considering the electrical properties for FGP plate reduces the normalized central deflection.In figures 14, the effect of electrical loading condition on the FGP plate responses is plotted. Results or determined in(l_1/4,l_2/4,z). Comparing the presented results with the previous figures for the mechanical loading shows that loading conditions affect thee FGP plate responses.

6. Conclusion

The higher-order shear and normal deformable plate theory was developed for determining the static responses of simply supported functionally graded piezoelectric rectangular plate subjected to mechanical and electrical loadings.

It was shown that obtained results from the presented theory are closed to the three dimensional elasticity solutions while where the solution procedure is simpler in comparison with the elasticity solution. Numerical results show that for thick FGP plates results converge for the fifth order of Legendre polynomials. Also, it was shown that for FGP plates, neutral plane does not coincide with the mid-plane. In addition, it was shown that electrical properties reduce the FGP plate stiffness.

References

Askari Farsangi, M.A. and Saidi, A.R. (2012) "Levy type solution for free vibration analysis of functionally graded rectangular plates with piezoelectric layers", *Smart Mater. Struct.,* **21**, 1-15. https://doi.org/10.1088/0964-1726/21/9/094017.

Batra, R.C. (2007) "Higher-order shear and normal deformable theory for functionally graded incompressible linear elastic plates", *Thin-Wall. Struct.*, **45**, 974–982. https://doi.org/10.1016/j.tws.2007.07.008.

Batra, R. and Vidoli, S. (2002) "Higher order piezoelectric plate theory derived from a three-dimensional variational principle", *AIAA J.*, **40**, 91–104. https://doi.org/10.2514/2.1618.

Behjat, B. and Khoshravan, M.R. (2012) "Geometrically nonlinear static and free vibration analysis of functionally graded piezoelectric plates", *Compos. Struct.*, **94**, 874–882. https://doi.org/10.1016/j.compstruct.2011.08.024.

Behjat, B., Salehi, M., Armina, A., Sadighi, M. and Abbasi, M. (2011) "A static and dynamic analysis of functionally graded piezoelectric plates under mechanical and electrical loading", *Scientia Iranica B*, **18**, 986–994. https://doi.org/10.1016/j.scient.2011.07.009.

Bodaghi, M. and Shakeri, M. (2012) "An analytical approach for free vibration and transient response of functionally graded piezoelectric cylindrical panels subjected to impulsive loads", *Compos. Struct.,* **94**, 1721-1735. https://doi.org/10.1016/j.compstruct.2012.01.009.

Chen, W.Q. and Ding, H.J. (2002) "On free vibration of a functionally graded piezoelectric rectangular plate", *Acta Mech.,* **153**, 207–216. https://doi.org/10.1007/BF01177452.

E. Mohseni, Saidi, A.R. and Mohammadi M. (2016) "Bending-stretching analysis of thick functionally graded micro-plates

using higher-order shear and normal deformable plate theory", *Mech. Adv. Mater. Struct.*, **24**, 1221-1230. https://doi.org/10.1080/15376494.2016.1227503.

Heyliger, P.R. and Ramirez, G. (2000) "Free vibration of laminated circular piezoelectric plates and discs", *Sound Vib.*, **229**, 935–956. https://doi.org/10.1006/jsvi.1999.2520.

Huang, X., Sun, J. and Li, J. (2015) "Effect of Initial Residual Stress and Machining-Induced Residual Stress on the Deformation of Aluminium alloy Plate", *J. Mech. Eng.*, **61**, 131-137.

Jadhav, P. and Bajoria, K. (2013) "Stability analysis of piezoelectric FGM plate subjected to electro-mechanical loading using finite element method", *Int. J. Appl. Sci. Eng.*, **11**, 375–391. http://dx.doi.org/10.6703%2fIJASE.2013.11(4).375.

Jam, J.E. and Nia, N.G. (2012) "Dynamic analysis of FGPM annular plate based on the 3-D theory of elasticity", *Int. J. Compos Mater.,* **2**, 53–62.

Lim, C.W. and He, L.H. (2001) "Exact solution of a compositionally graded piezoelectric layer under uniform stretch, bending and twisting", *Int. J. Mech. Sci*., **43**, 2479–2492. https://doi.org/10.1016/S0020-7403(01)00059-5.

Lu, P., Lee, H.P. and Lu, C. (2005) "An exact solution for functionally graded piezoelectric laminates in cylindrical bending", *Int. J. Mech. Sci.,* **12**, 437–458. https://doi.org/10.1016/j.ijmecsci.2005.01.012.

Mindlin, R.D., Schaknow, A. and Deresiewicz, H. (1856) "Flexural vibration of rectangular plates", *J. Appl. Mech.*, **23**, 430-436.

Mohammadi, M., Mohseni, E. and Moeinfar, M. (2019) "Bending, buckling and free vibration analysis of incompressible functionally graded plates using higher order shear and normal deformable plate theory", *Appl. Math. Model.,* **69**, 47-62. https://doi.org/10.1016/j.apm.2018.11.047.

Nazari, M.B., Shariati, M., Eslami, M.R. and Hassani, B. (2011) "Computation of stress intensity factor in functionally graded plates under thermal shock", *J. Mech. Eng.*, **57**, 622-632.

Reddy, J.N. (1984). "A simple higher-order theory for laminated composite plates", *Appl. Mech.*, **45**, 745–752. https://doi.org/10.1115/1.3167719.

Reissner, E. (1994) "On the theory of bending of elastic plates", *J. Math. Phys.*, **23**, 184-191. https://doi.org/10.1002/sapm1944231184.

Sheikholeslami, S.A. and Saidi, A.R. (2013) "Vibration analysis of functionally graded rectangular plates resting on elastic foundation sing higher-order shear and normal deformable plate theory", *Compos. Struct.*, **106**, 350-361. https://doi.org/10.1016/j.compstruct.2013.06.016.

Wang, J. and Yang, J. (2000) "Higher-order theories of piezoelectric plates and applications", *Appl. Mech. Rev.*, **53**, 87-99. https://doi.org/10.1115/1.3097341.

Wattanasakulponga, N. and Chaikittiratanab, A. (2015) "Exact solutions for static and dynamic analyses of carbon nanotube-reinforced composite plates with Pasternak elastic foundation", *Appl. Math. Model.*, **39**, 5459–5472. https://doi.org/10.1016/j.apm.2014.12.058.

Wu, X.H., Chen, C.Q., Shen, Y.P. and Tian, X.G.A. (2002) "High order theory for functionally graded piezoelectric shells", *Int. J. Solids Struct.*, **4**, 5325–5344. https://doi.org/10.1016/S0020-7683(02)00418-3.

Xiang, H.J. and Shi, Z.F. (2009) "Static analysis for functionally graded piezoelectric actuators or sensors under a combined electro-thermal load", *Eur. J. Mech. A Solids*, **28**, 338–346. https://doi.org/10.1016/j.euromechsol.2008.06.007.

Zhong, Z. and Shang, E.T. (2003) "Three-dimensional exact analysis of a simply supported functionally gradient piezoelectric plate", *Int. J. Solids Struct.*, **40**, 5335–5352. https://doi.org/10.1016/S0020-7683(03)00288-9.

Zhong Z. and Tao Y.U. (2006) "Vibration of simply supported functionally graded piezoelectric rectangular plate", *Smart Mater. Struct.*, **15**, 1726-1741. https://doi.org/10.1088/0964-1726/15/5/029.

CC

Appendix A: Simplified governing equilibrium equations of simply supported FGP plate

According to the Navier solution for simply supported FGP plate, governing equilibrium equations are simplified as

$$\tilde{V}_1^{cmn}\left\{-\int_{-\frac{h}{2}}^{\frac{h}{2}} L_a L_c C_{11} dz\left[(\frac{m\pi}{l_1})^2+\frac{1}{2}(\frac{n\pi}{l_2})^2\right]+\frac{1}{2}\int_{-\frac{h}{2}}^{\frac{h}{2}} L_a L_c C_{12} dz\left[(\frac{n\pi}{l_2})^2\right]\right\}-D_{ab}D_{cd}\int_{-\frac{h}{2}}^{\frac{h}{2}} L_b L_d C_{55} dz$$
$$+\tilde{V}_2^{cmn}\left\{-\frac{1}{2}\int_{-\frac{h}{2}}^{\frac{h}{2}} L_a L_c C_{11} dz\left[(\frac{m\pi}{l_1})(\frac{n\pi}{l_2})\right]-\frac{1}{2}\int_{-\frac{h}{2}}^{\frac{h}{2}} L_a L_c C_{12} dz\left[(\frac{m\pi}{l_1})(\frac{n\pi}{l_2})\right]\right\}+\tilde{\varphi}\left\{-\int_{-\frac{h}{2}}^{\frac{h}{2}} L_a e_{31}\left[\frac{8z}{h^2}\right]dz\left[(\frac{m\pi}{l_1})\right]\right.$$
$$\left.-D_{ab}\int_{-\frac{h}{2}}^{\frac{h}{2}} L_b e_{15}\left[1-\left(\frac{2z}{h}\right)^2\right]dz\left[(\frac{m\pi}{l_1})\right]\right\}+\tilde{W}^{dmn}\left\{D_{dc}\int_{-\frac{h}{2}}^{\frac{h}{2}} L_a L_c C_{13} dz\left[(\frac{m\pi}{l_1})\right]-D_{ab}\int_{-\frac{h}{2}}^{\frac{h}{2}} L_b L_d C_{55} dz\left[(\frac{m\pi}{l_1})\right]\right\}$$
$$+\left[(\frac{m\pi}{l_1})\right]\int_{-\frac{h}{2}}^{\frac{h}{2}} L_a e_{31} dz\left[\tilde{A}^{mn}\right]-\left[(\frac{m\pi}{l_1})\right]D_{ab}\int_{-\frac{h}{2}}^{\frac{h}{2}} L_b e_{15} z dz\left[\tilde{A}^{mn}\right]-\left[(\frac{m\pi}{l_1})\right]D_{ab}\int_{-\frac{h}{2}}^{\frac{h}{2}} L_b e_{15} dz\left[\tilde{B}^{mn}\right]=0$$

A-1

$$\tilde{V}_1^{cmn}\left\{-\frac{1}{2}\int_{-\frac{h}{2}}^{\frac{h}{2}} L_a L_c C_{11} dz\left[(\frac{m\pi}{l_1})(\frac{n\pi}{l_2})\right]-\frac{1}{2}\int_{-\frac{h}{2}}^{\frac{h}{2}} L_a L_c C_{12} dz\left[(\frac{m\pi}{l_1})(\frac{n\pi}{l_2})\right]\right\}+\tilde{V}_2^{cmn}\left\{-\int_{-\frac{h}{2}}^{\frac{h}{2}} L_a L_c C_{11} dz\left[\frac{1}{2}(\frac{m\pi}{l_1})^2+(\frac{n\pi}{l_2})^2\right]\right.$$
$$\left.+\frac{1}{2}\int_{-\frac{h}{2}}^{\frac{h}{2}} L_a L_c C_{12} dz\left[(\frac{m\pi}{l_1})^2\right]-D_{ab}D_{cd}\int_{-\frac{h}{2}}^{\frac{h}{2}} L_b L_d C_{55} dz\right\}+\tilde{W}^{dmn}\left\{D_{dc}\int_{-\frac{h}{2}}^{\frac{h}{2}} L_a L_c C_{13} dz\left[(\frac{n\pi}{l_2})\right]-D_{ab}\int_{-\frac{h}{2}}^{\frac{h}{2}} L_b L_d C_{55} dz\left[(\frac{n\pi}{l_2})\right]\right\}$$
$$+\tilde{\varphi}\left\{-\int_{-\frac{h}{2}}^{\frac{h}{2}} L_a e_{31}\left[\frac{8z}{h^2}\right]dz\left[(\frac{n\pi}{l_2})\right]-D_{ab}\int_{-\frac{h}{2}}^{\frac{h}{2}} L_b e_{15}\left[1-\left(\frac{2z}{h}\right)^2\right]dz\left[(\frac{n\pi}{l_2})\right]\right\}$$
$$+\left[(\frac{n\pi}{l_2})\right]\int_{-\frac{h}{2}}^{\frac{h}{2}} L_a e_{31} dz\left[\tilde{A}^{mn}\right]-\left[(\frac{n\pi}{l_2})\right]D_{ab}\int_{-\frac{h}{2}}^{\frac{h}{2}} L_b e_{15} z dz\left[\tilde{A}^{mn}\right]-\left[(\frac{n\pi}{l_2})\right]D_{ab}\int_{-\frac{h}{2}}^{\frac{h}{2}} L_b e_{15} dz\left[\tilde{B}^{mn}\right]=0$$

A-2

$$\tilde{V}_1^{cmn}\left\{-\int_{-\frac{h}{2}}^{\frac{h}{2}} L_a L_d C_{55} dz\left[D_{cd}(\frac{m\pi}{l_1})\right]+D_{ab}\int_{-\frac{h}{2}}^{\frac{h}{2}} L_b L_c C_{13} dz\left[(\frac{m\pi}{l_1})\right]\right\}+\tilde{V}_2^{cmn}\left\{-\int_{-\frac{h}{2}}^{\frac{h}{2}} L_a L_d C_{55} dz\left[D_{cd}(\frac{n\pi}{b})\right]\right.$$
$$\left.+D_{ab}\int_{-\frac{h}{2}}^{\frac{h}{2}} L_b L_c C_{13} dz\left[(\frac{n\pi}{l_2})\right]\right\}+\tilde{W}^{dmn}\left\{-\int_{-\frac{h}{2}}^{\frac{h}{2}} L_a L_d C_{55} dz\left[(\frac{m\pi}{l_1})^2+(\frac{n\pi}{l_2})^2\right]-D_{ab}\int_{-\frac{h}{2}}^{\frac{h}{2}} L_b L_d C_{55} dz\left[(\frac{m\pi}{l_1})\right]-D_{ab}D_{cd}\int_{-\frac{h}{2}}^{\frac{h}{2}} L_b L_d C_{55} dz\right\}$$
$$+\tilde{\varphi}\left\{-\int_{-\frac{h}{2}}^{\frac{h}{2}} L_a e_{15}\left[1-\left(\frac{2z}{h}\right)^2\right]dz\left[(\frac{m\pi}{l_1})^2+(\frac{n\pi}{l_1})^2\right]+D_{ab}\int_{-\frac{h}{2}}^{\frac{h}{2}} L_b e_{33}\left[\frac{8z}{h^2}\right]dz\right\}$$
$$+\left[(\frac{m\pi}{l_1})^2+(\frac{n\pi}{l_1})^2\right]\int_{-\frac{h}{2}}^{\frac{h}{2}} L_a e_{15} z dz\left[\tilde{A}^{mn}\right]+\left[(\frac{m\pi}{l_1})^2+(\frac{n\pi}{l_1})^2\right]\int_{-\frac{h}{2}}^{\frac{h}{2}} L_a e_{15} dz\left[\tilde{B}^{mn}\right]-D_{ab}\int_{-\frac{h}{2}}^{\frac{h}{2}} L_b e_{33} dz\left[\tilde{A}^{mn}\right]+P(x,y)L_a(\frac{-h}{2})=0$$

A-3

$$\tilde{V}_1^{cmn}\left\{-\int_{-\frac{h}{2}}^{\frac{h}{2}} L_d e_{15} dz\left[D_{cd}(\frac{m\pi}{l_1})\right]-\int_{-\frac{h}{2}}^{\frac{h}{2}} L_c\frac{\partial e_{31}}{\partial z}dz\left[(\frac{m\pi}{l_1})\right]\right\}$$
$$+\tilde{V}_2^{cmn}\left\{-\int_{-\frac{h}{2}}^{\frac{h}{2}} L_d e_{15} dz\left[D_{cd}(\frac{n\pi}{l_1})\right]-\int_{-\frac{h}{2}}^{\frac{h}{2}} L_d e_{31} dz\left[D_{cd}(\frac{n\pi}{l_2})\right]-\int_{-\frac{h}{2}}^{\frac{h}{2}} L_c\frac{\partial e_{31}}{\partial z}dz\left[(\frac{n\pi}{l_2})\right]\right\}$$
$$+\tilde{W}^{dmn}\left\{-\int_{-\frac{h}{2}}^{\frac{h}{2}} L_d e_{15} dz\left[(\frac{m\pi}{l_1})^2+(\frac{n\pi}{l_2})^2\right]+D_{bc}D_{db}\int_{-\frac{h}{2}}^{\frac{h}{2}} L_c e_{33} dz\left[(\frac{m\pi}{l_1})\right]+D_{dc}\int_{-\frac{h}{2}}^{\frac{h}{2}} L_c\frac{\partial e_{33}}{\partial z}dz\right\}+\tilde{\varphi}\left\{\int_{-\frac{h}{2}}^{\frac{h}{2}}\lambda_{11}\left[1-\left(\frac{2z}{h}\right)^2\right]dz\left[(\frac{m\pi}{l_1})^2+(\frac{n\pi}{l_2})^2\right]\right.$$
$$\left.+\int_{-\frac{h}{2}}^{\frac{h}{2}}\lambda_{33}dz\left[\frac{8}{h^2}\right]+\int_{-\frac{h}{2}}^{\frac{h}{2}}\frac{\partial\lambda_{33}}{\partial z}dz\left[\frac{8z}{h^2}\right]\right\}-\left[(\frac{m\pi}{l_1})^2+(\frac{n\pi}{l_2})^2\right]\int_{-\frac{h}{2}}^{\frac{h}{2}}\lambda_{11} z dz\left[\tilde{A}^{mn}\right]-\left[(\frac{m\pi}{l_1})^2+(\frac{n\pi}{l_2})^2\right]\int_{-\frac{h}{2}}^{\frac{h}{2}}\lambda_{11} dz\left[\tilde{B}^{mn}\right]-\int_{-\frac{h}{2}}^{\frac{h}{2}}\frac{\partial\lambda_{33}}{\partial z}dz\left[\tilde{A}^{mn}\right]=0$$

A-4